Specific heat of quantum-spin chains: Application to $(C_6H_{11}NH_3)CuBr_3$ and $(C_6H_{11}NH_3)CuCl_3$

L. S. Campana, A. Caramico D'Auria, U. Esposito, and G. Kamieniarz*
Dipartimento di Scienze Fisiche, Università di Napoli, piazzale V. Tecchio, 80, 80125 Napoli, Italy
(Received 28 September 1989)

A real-space renormalization-group (RSRG) approach and numerical calculations are applied in order to study the specific heat of $(C_6H_{11}NH_3)CuBr_3$ and $(C_6H_{11}NH_3)CuCl_3$, which are built up of the ferromagnetic spin-$\frac{1}{2}$ quantum chains and are described by anisotropic Heisenberg models. As to the RSRG approach, our previous zero-field easy-plane calculations are extended to the XYZ model in the presence of a magnetic field, and qualitative agreement with experiment is found, especially in the appearance of the soliton peaks in the in-plane excess specific heat. Imposing free boundary conditions, the finite-size numerical results are applied to chains with length $N \leq 12$ and extrapolated for $1/N \to 0$. Good convergence for most temperatures is found, and agreement with experiment is concluded.

I. INTRODUCTION

Quasi-one-dimensional magnetic systems have been the subject of great interest in recent years.[1] The best realizations of these systems, for spin-$\frac{1}{2}$ ferromagnetic chains, are $(C_6H_{11}NH_3)CuCl_3$, and its bromine isomorph, abbreviated as CHAC and CHAB, respectively.[2] These compounds are made of weakly coupled chains, the interchain coupling J' being of three orders of magnitude lower than the intrachain coupling. The interaction J' is responsible for three-dimensional antiferromagnetic ordering below the transition temperature, which is $T_c = 2.21$ K for CHAC and $T_c = 1.50$ K for CHAB. If we neglect the interchain interaction, both compounds are well represented, in presence of an external field $\mathbf{B}$, by the Hamiltonian:

$$H = -2\sum_j (J^x s_j^x s_{j+1}^x + J^y s_j^y s_{j+1}^y + J^z s_j^z s_{j+1}^z) - g\mu_B \mathbf{B}\cdot\sum_j \mathbf{s}_j \ . \tag{1}$$

In this paper an external field will be taken into account only for CHAB ($g = 2.01$).

As is well known, the low-temperature thermodynamic properties of one-dimensional systems are strongly affected by the presence of anisotropies.[1,3] The absolute values of the anisotropies have been found from ferromagnetic resonance experiments[4] which, combined with specific-heat measurements,[2] give for CHAB a 5% easy-plane anisotropy with

$$J^x/k_B = 55.92, \quad J^y/k_B = 55.91, \quad J^z/k_B = 53.18 \ , \tag{2}$$

all in K, whereas for the CHAC an orthorhombic anisotropy with

$$J^x/k_B = 45.52, \quad J^y/k_B = 44.99, \quad J^z/k_B = 44.49 \ , \tag{3}$$

also in K. Some uncertainty, however, still remains about the values of the exchange parameters. On one hand, recent experiments[5] by inelastic neutron scattering gave $J^x/k_B = 67 \pm 1$ K for CHAB; on the other hand, new specific-heat measurements[6] at higher fields for CHAB yielded the values in K

$$J^x/k_B = J^y/k_B = 63, \quad J^z/k_B = 60.25 \tag{4}$$

with small anisotropy inside the easy (X-Y) plane neglected. Because we are interested in the specific heat, we assume in this paper the values (4) for CHAB and (3) for CHAC.

In the presence of the magnetic field applied within the easy (XY) plane, the Hamiltonian for the CHAB can be mapped onto a sine-Gordon Hamiltonian[7,8] if one considers the limit of classical spins and large anisotropy and the continuum limit. As a consequence, the specific heat of the system has been investigated in terms of solitonlike excitations, and a large amount of work has been done in this direction,[9–12] taking into account quantum effects and out-of-plane fluctuations. However, until now, the effect of the various approximations involved in the mapping of the original Hamiltonian onto the sine-Gordon one is not clear. For this reason it is interesting to calculate the specific heat of CHAB following different approaches, including some numerical techniques. The specific heat of the model (1) with the parameters (2) has been evaluated[13] by extrapolation of numerical results for finite chains up to $N = 10$ sites. The partition function of the one-dimensional quantum system (1) has been mapped onto the partition function of a classical two-dimensional model via the Trotter-Suziki transformation and has been evaluated by means of Monte Carlo or transfer-matrix techniques.[14–16]

In the previous paper[17] we have obtained the specific heat in zero field for an XXZ chain that is appropriate for CHAB, via a real-space renormalization-group approach. In this paper we consider a renormalization-group approach to an XYZ chain in an external field, which can describe CHAB and CHAC simultaneously. This is the subject of Sec. II, which also includes some zero-field numerical results for CHAC.

In Sec. III we present the results for the excess specific heat of CHAB at higher fields obtained via finite-size calculations for chains up to $N=12$ sites. Linear and parabolic extrapolations are performed to infinite chain. In Sec. IV the results are discussed and some conclusions are presented.

II. RENORMALIZATION-GROUP SCHEME

In the presence of a magnetic field applied along the x direction (which lies in the easy plane for CHAB) the Hamiltonian for XYZ chain can be written

$$\beta H=\mathcal{H}=-\tfrac{1}{2}\sum_j\sum_\alpha K^\alpha\sigma_j^\alpha\sigma_{j+1}^\alpha-\tfrac{1}{2}h\sum_j\sigma_j^x \ . \tag{5}$$

Here $\alpha\equiv(x,y,z)$, σ_j^α stands for Pauli spin-$\frac{1}{2}$ operators, and

$$\beta=1/k_BT,\ K^\alpha=\beta J^\alpha,\ h=\beta g\mu_B B \ . \tag{6}$$

Our renormalization scheme is based on the division of the chain into cells of three sites; we attribute a (Pauli) cell spin $\mathbf{S}_i$ to each cell; then the renormalization transformation, which preserves the free energy, is defined by

$$\exp[-\mathcal{H}'(\mathbf{S})]=\mathrm{Tr}_\sigma\exp[-\mathcal{H}(\sigma)]P(\mathbf{S},\sigma) \ , \tag{7}$$

where $P(\mathbf{S},\sigma)$ is an appropriate weight operator. As before[17,18] we choose it in the form

$$P(\mathbf{S},\sigma)=\prod_i\tfrac{1}{2}[1+\tfrac{1}{2}\mathbf{S}_i\cdot\mathbf{M}(\sigma_{\mathrm{im}})] \ , \tag{8}$$

where i is a cell index, $m=1,2,3$ denotes one of the three sites of a cell, and

$$\mathbf{M}(\sigma_{\mathrm{im}})=\sigma_{i1}+\sigma_{i2}+\sigma_{i3}-\tfrac{1}{3}[\sigma_{i1}(\sigma_{i2}\cdot\sigma_{i3})+\sigma_{i3}(\sigma_{i1}\cdot\sigma_{i2})+\sigma_{i2}(\sigma_{i3}\cdot\sigma_{i1})] \ . \tag{9}$$

We divide the Hamiltonian into an intracell term $\mathcal{H}_0$, which includes also the external field, and an intercell term V. Next, we expand Eq. (7) in terms of V using the Feynman expansion[19] up to the first order. However, proceeding in the standard way, we obtain a zero-order renormalized Hamiltonian of the form

$$\mathcal{H}_0'=-N'E_0'-\tfrac{1}{2}h_0'\sum_i S_i^x,\quad N'=N/3 \ , \tag{10}$$

which is not a multiple of the unit operator. This fact is due to the presence, inside the free cell Hamiltonian, of the symmetry-breaking term associated with the external field. As a consequence,[20] the expansion should be made with great care in order to take into account the noncommutativity of the operators and to avoid the appearance of non-Hermitian terms. First, we write

$$\exp[-2\mathcal{H}']=\mathrm{Tr}[\exp(-\mathcal{H})P]\mathrm{Tr}[P\exp(-\mathcal{H})] \ . \tag{11}$$

For simplicity in (11) we have omitted the indication of the site and cell spins. Next we consider the renormalized Hamiltonian as a sum of a zero-order term $\mathcal{H}_0'$ and a first-order term $\mathcal{H}_1'$, and we expand both sides of (11) via the Feynman formula up to the first order. The left-hand side expansion gives

$$e^{-2\mathcal{H}'}=e^{-2\mathcal{H}_0'}-e^{-\mathcal{H}_0'}\left[\int_0^1 dv\, e^{v\mathcal{H}_0'}\mathcal{H}_1'e^{-v\mathcal{H}_0'}+\mathrm{H.c.}\right]e^{-\mathcal{H}_0'} \ , \tag{12}$$

whereas the right-hand side gives

$$\mathrm{Tr}[\exp(-\mathcal{H})P]\mathrm{Tr}[P\exp(-\mathcal{H})]=(\mathrm{Tr}e^{-\mathcal{H}_0}P)(\mathrm{Tr}Pe^{-\mathcal{H}_0})-\left[(\mathrm{Tr}e^{-\mathcal{H}_0}P)\int_0^1 d\mu\,\mathrm{Tr}(Pe^{-\mu\mathcal{H}_0}Ve^{\mu\mathcal{H}_0}e^{-\mathcal{H}_0})+\mathrm{H.c.}\right] \ . \tag{13}$$

Equating zero-order and first-order terms we recover Eq. (10) and

$$\int_0^1 d\nu\, e^{\nu\mathcal{H}_0'}\mathcal{H}_1'e^{-\nu\mathcal{H}_0'}+\mathrm{H.c.}=\int_0^1 d\mu\,\mathrm{Tr}(Pe^{-\mu\mathcal{H}_0}Ve^{\mu\mathcal{H}_0}e^{-\mathcal{H}_0})(\mathrm{Tr}e^{-\mathcal{H}_0}P)^{-1}+\mathrm{H.c.} \tag{14}$$

Following this procedure Hermiticity is automatically satisfied. We look for a solution of (14) in the form

$$\mathcal{H}_1'=-N'E_1'-\tfrac{1}{2}h_1'\sum_i S_i^x-\tfrac{1}{2}\sum_i\sum_\alpha K'^\alpha S_i^\alpha S_{i+1}^\alpha \ . \tag{15}$$

After a straightforward calculation we obtain solutions for the parameters E_1', h_1', and K'^α. Adding up (10) and (15) we obtain a renormalized Hamiltonian $\mathcal{H}'$, which preserves the original form (5), a part from a constant factor

$$\mathcal{H}'=-N'E'-\tfrac{1}{2}h'\sum_i S_i^x-\tfrac{1}{2}\sum_i\sum_\alpha K'^\alpha S_i^\alpha S_{i+1}^\alpha \ . \tag{16}$$

Explicit expressions for the recursion relations that link old and new parameters are given in the Appendix.

The renormalization process can be iterated. Let $E^{(n)}$ be the constant that appears at the nth step of the renormalization procedure. Summing up all the constant terms we obtain in the standard way the dimensionless free energy per spin

$$f=\sum_{m=1}^{\infty}E^{(n)}/3^n \tag{17}$$

in terms of which the specific heat per site in units of k_B can be expressed by

$$C=\beta^2\partial^2 f/\partial\beta^2 \ . \tag{18}$$

We have presented in a previous paper[17] the zero-field specific-heat results for CHAB, which shows easy-plane anisotropy. It is of interest to compare the experimental zero-field specific-heat data for CHAC with the results obtained here for the XYZ-type system. Our renormalization-group (RG) predictions are reported in Fig. 1. They show good agreement with experimental data for $T>7$ K. The experimental peak present at low

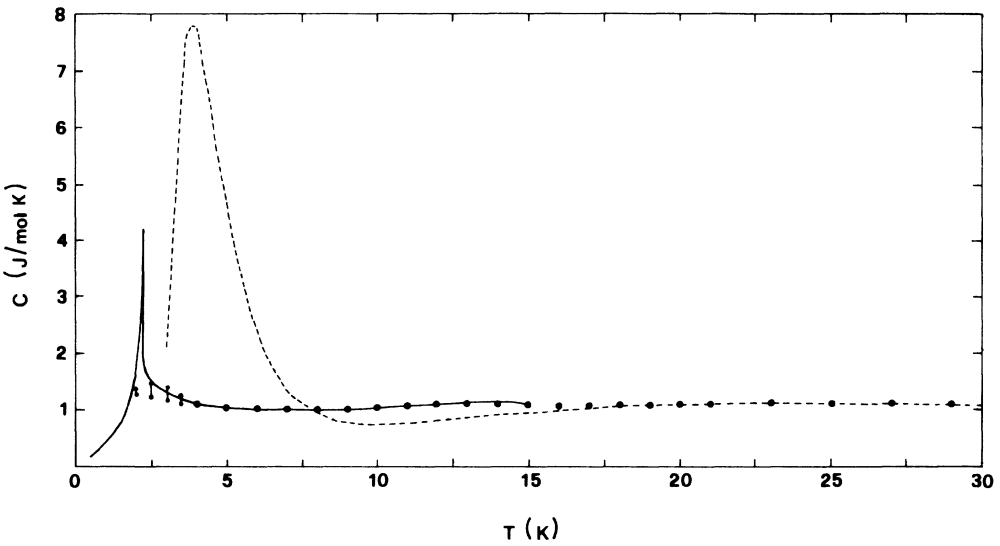

FIG. 1. Specific heat of CHAC in molar units. The experimental and renormalization-group results are denoted using solid and dashed lines, respectively. Numerical results by extrapolation of finite chains (Sec. III) are shown by solid circles or by intercepts when linear and parabolic extrapolations do not coincide.

temperature is associated with the three-dimensional ordering so that the peak obtained here at the first-order expansion is spurious. In Fig. 1, we present also numerical results for CHAC obtained by extrapolation of finite chains, which will be discussed in Sec. III.

Now we turn our attention to the XXZ-type system, which is appropriate for CHAB. We have calculated the specific heat as a function of temperature for different values of the applied field. The excess specific heat $\Delta C(T,B)=C(T,B)-C(T,0)$ as a function of T displays a maximum for any value of the field. A comparison is made with the recent high-field experiments.[6] The result

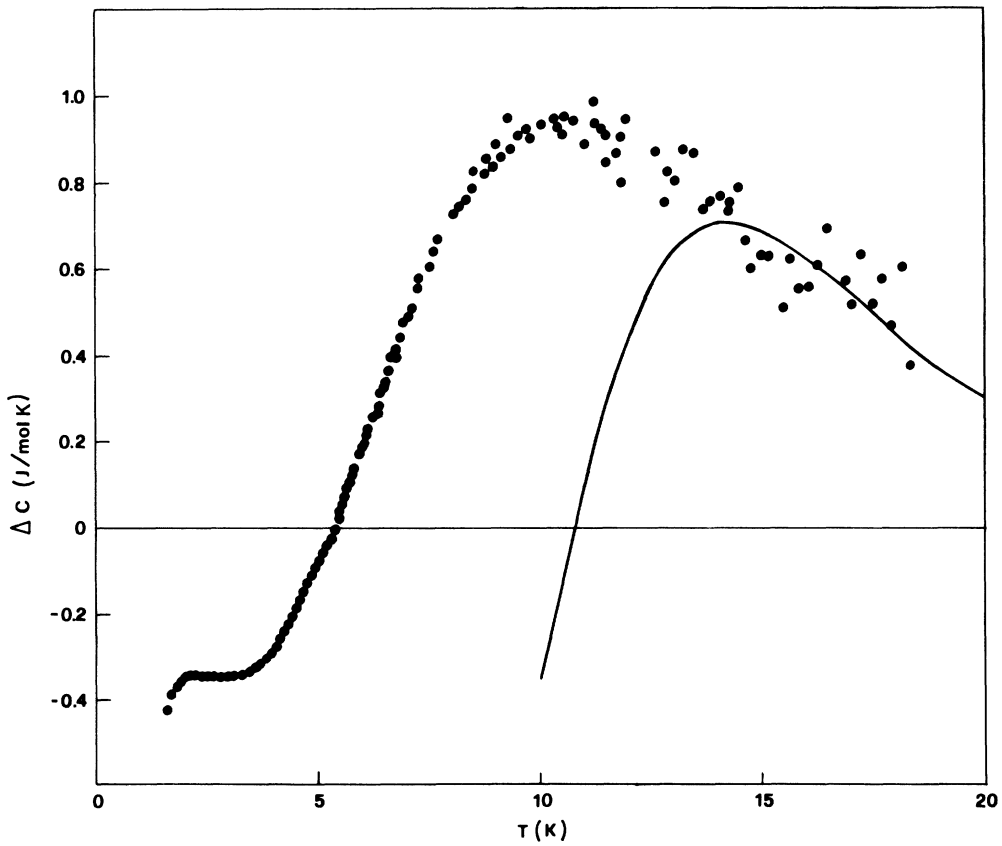

FIG. 2. Excess specific heat for CHAB in molar units for $B=2$ T. The experimental data are shown using solid points, the renormalization-group results using the solid line.

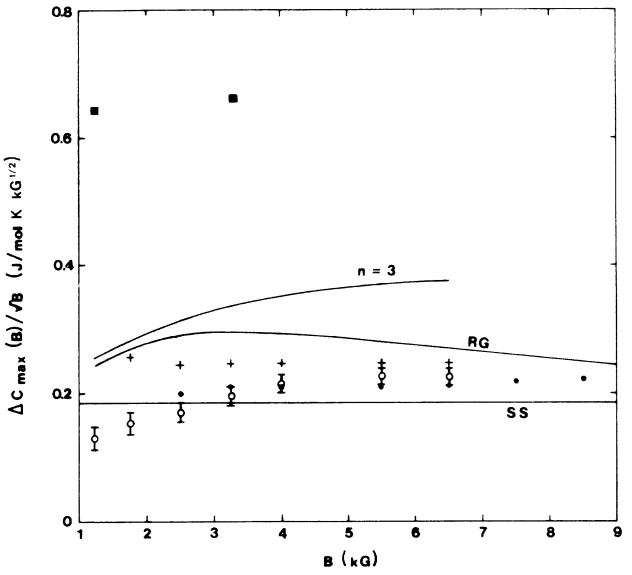

FIG. 3. Height $\Delta C_{\max}/\sqrt{B}$ of the peak in the molar excess specific heat vs the external field for CHAB. Experimental data are shown using open circles with error bars. Our results are shown using the curve denoted RG. Solid points and crosses represent numerical calculations of Refs. 13 and 16, respectively. The lines $n=3$ and SS represent exact results for the classical spin model and for the sine-Gordon model. Solid squares represent the semiclassical approach of Ref. 12.

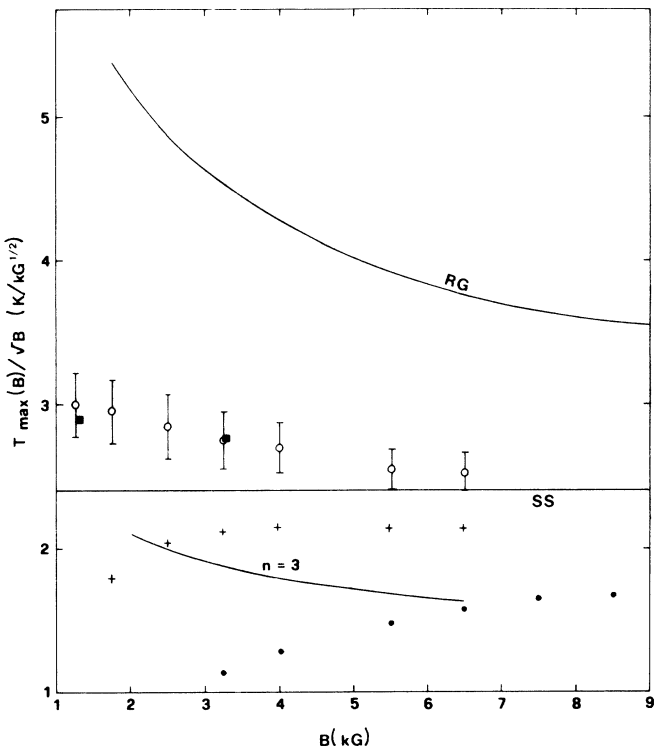

FIG. 4. Peak positions $T_{\max}/\sqrt{B}$ in the molar excess specific heat vs the external field for CHAB. The notations are the same as in Fig. 3.

for $B=2$ T is shown in Fig. 2. The qualitative behavior is correct, although the maximum is shifted towards higher temperatures and its height is underestimated. Similar results are obtained for $B=1$ and 3 T.

According to the sine-Gordon (sG) model the quantity $\Delta C/\sqrt{B}$, as a function of $T/\sqrt{B}$, shows universal behavior.[21] As a consequence, the peak positions and their heights expressed in reduced units, $T_{\max}/\sqrt{B}$ and $\Delta C_{\max}/\sqrt{B}$, should assume a constant value. Experimental data,[10] however, do not show this behavior. In Fig. 3 the curve labeled RG presents our results for the peak values with the external field in the range 1.25–9 kG. Experimental data are reported using open circles with error bars. The constant value predicted by the sG theory is shown by the line SS, after Schneider and Stoll.[21] As we shall see, our results do not assume a constant value and are in reasonable agreement with experiments. The increase of $\Delta C_{\max}/\sqrt{B}$ with the field, which is not recovered within the sG theory, is due to the out-of-plane spin fluctuations. This fact is concluded from a good qualitative behavior of the curve $n=3$, which describes a chain of three component classical spins.[22] The numerical finite-size[13] results (solid points) are rather close to the experimental data, while the quantum transfer matrix results[16] (crosses) nearly reproduce a constant value.

For the peak positions the agreement with experimental data is less accurate, apart from the results of Fogedby,[12] as shown in Fig. 4. Note that the curves RG and $n=3$ reproduce the qualitative behavior of the experimental data, in contrast with numerical results.[13,16]

III. NUMERICAL APPROACH

Here we extend the previous numerical finite-size calculations[13] for the chains up to $N=12$ sites. As before, we impose the free boundary conditions and, additionally, we utilize the symmetries of the Hamiltonian (1) with respect to the reflection of the z axis and to the inversion of the chain. These symmetries enable us to find four invariant subspaces so that the largest size of the matrix we have to diagonalize for $N=12$ amounts to 1056×1056.

Having found the eigenvalues E_i of the matrix representation of the Hamiltonian (1), we evaluate the specific heat $C(T,B)$ in molar units by the formula

$$C_N=\frac{R}{N}(\langle E^2\rangle-\langle E\rangle^2)/(k_BT)^2\ , \tag{19}$$

where

$$\langle A\rangle=\left[\sum_i A_i\exp(-E_i/k_BT)\right]\Big/\left[\sum_i\exp(-E_i/k_BT)\right] \tag{20}$$

and R is the gas constant. The quantities C_N depend on the number N of spins in the chain, so that we analyze them as a function of $1/N$ and we perform extrapolations for $1/N\to0$.

Experiments on CHAB have been performed in a constant field. The essential feature of the excess specific heat $\Delta C(T,B)$ data[6,10] is the appearance of peaks that we recover in our calculations. However, before presenting

TABLE I. Extrapolated values of $C(T,B)$ and $\Delta C(T,B)$ vs the number of points n at the peak position $T_{max}(B)=7.5$ K for $B=1$ T. The superscripts l and p refer to the linear and parabolic extrapolations, respectively.

n	C^l	ΔC^l	C^p	ΔC^p
2	1.8499	0.6130		
3	1.8388	0.6008	1.9546	0.7283
4	1.8259	0.5864	1.9481	0.7222
5	1.8061	0.5698	1.9669	0.7115
6	1.7738	0.5512	1.9996	0.6938
7	1.7389	0.5302	1.9708	0.6715
8	1.7363	0.5048	1.8156	0.6497
9	1.7692	0.4714	1.6812	0.6262
10	1.7217	0.4300	1.8298	0.5856
11	1.5312	0.3809	1.9694	0.5209

TABLE III. Extrapolated values of $C(T,B)$ and $\Delta C(T,B)$ vs the number of points n at a temperature greater than the peak position ($T=15$ K, $B=1$ T). The superscripts l and p denote the estimates from the linear and parabolic extrapolations, respectively.

n	C^l	ΔC^l	C^p	ΔC^p
2	1.2857	0.1547		
3	1.2826	0.1516	1.3151	0.1843
4	1.2788	0.1480	1.3140	0.1823
5	1.2744	0.1438	1.3120	0.1796
6	1.2701	0.1389	1.3045	0.1760
7	1.2655	0.1331	1.2974	0.1714
8	1.2516	0.1263	1.3172	0.1650
9	1.2346	0.1185	1.3111	0.1561
10	1.2810	0.1088	1.1728	0.1457
11	1.2855	0.0961	1.2528	0.1315

our results, let us comment on our extrapolation procedure.

In Tables I and II we show the dependence of the extrapolated data on the number of points n and on the type of extrapolation at the peak position $T_{max}(B)$. Linear (denoted by l) and parabolic (denoted by p) extrapolations in $1/N$ are carried out. The meaning of n is the following: $n=2$ shows the estimates extrapolated from the last two points $N=11$ and 12; $n=3$ shows the estimates when $10\leq N\leq 12$, etc. If $n=11$, all the points with $2\leq N\leq 12$ are taken into account. The peak positions $T_{max}(B)$ appear at about 7.5 and 12.5 K for $B=1$ T and $B=3$ T, respectively, so that the extrapolations in the latter case are more reliable. At $T=7.5$ K (Table I), the linear and parabolic extrapolations yield different estimates of $C(7.5, 1)$ and $\Delta C(7.5, 1)$. The relative values C^l/C^p and $\Delta C^l/\Delta C^p$ amount to 0.95 and 0.84 for the first rows ($n=2$ for l and $n=3$ for p). If we consider only one type of extrapolation and assume $n<5$, we obtain uncertainty for $C(\Delta C)$ only on the third (second) significant digit; this fact suggests that in this case we have a better accuracy. Clearly, the quantity C is found with a better accuracy than the excess ΔC. If we propose to Table II ($T_{max}=12.5$ K, $B=3$ T), the corresponding ratios are 0.987 and 0.971, i.e., they are considerably improved with respect to those found from Table I.

Convergence of extrapolations is systematically improved with increasing temperatures. If we fix $B=1$ T, the corresponding results for $T=15$ K and $T=63$ K are reported in Tables III and IV, respectively. Clearly, the convergence in Table III is comparable to that in Table II. However, proceeding to Table IV, the convergence is remarkably improved. Practically, the estimates depend neither on the type of extrapolation nor on the number of points n. For this reason we assume the difference between the predictions of the linear and parabolic extrapolations as the estimates of the error bars.

In Fig. 5 we present our results for the excess specific heat. The experimental data on CHAB (Ref. 6) are denoted by open circles, solid circles, and crosses for $B=1,2,3$ T, respectively. Our estimates are represented by the intercepts that join the points we find from linear and parabolic extrapolations in $1/N$. If these intercepts cannot be visualized, we mark our predictions by triangles. We see that if the linear and parabolic extrapolations approximately coincide (the triangles), they are close to the experimental results even at low temperatures. We illustrate our results for $B=2$ T only at higher

TABLE II. Extrapolated values of $C(T,B)$ and $\Delta C(T,B)$ vs the number of points n at the peak position $T_{max}(B)=12$ K for $B=3$ T. The superscripts l and p refer to the linear and parabolic extrapolations, respectively.

n	C^l	ΔC^l	C^p	ΔC^p
2	2.2377	1.0947		
3	2.2340	1.0911	2.2726	1.1283
4	2.2286	1.0861	2.2783	1.1328
5	2.2215	1.0788	2.2805	1.1384
6	2.2120	1.0678	2.2812	1.1457
7	2.1941	1.0520	2.2999	1.1501
8	2.1598	1.0315	2.3300	1.1439
9	2.1374	1.0021	2.2627	1.1339
10	2.1576	0.9508	2.1349	1.1279
11	2.0494	0.8717	2.2804	1.0814

TABLE IV. Extrapolated values $C(T,B)$ and $\Delta C(T,B)$ vs the number of points n at high temperatures ($T=63.0$ K, $B=1$ T). The linear (l) and parabolic (p) extrapolations are considered.

n	C^l	ΔC^l	C^p	ΔC^p
2	1.077 410	0.003 251		
3	1.077 410	0.003 250	1.077 411	0.003 256
4	1.077 408	0.003 249	1.077 419	0.003 258
5	1.077 407	0.003 247	1.077 422	0.003 262
6	1.077 403	0.003 244	1.077 428	0.003 268
7	1.077 396	0.003 237	1.077 436	0.003 277
8	1.077 382	0.003 223	1.077 451	0.003 290
9	1.077 353	0.003 196	1.077 471	0.003 307
10	1.077 438	0.003 141	1.077 233	0.003 323
11	1.074 157	0.003 032	1.081 267	0.003 308

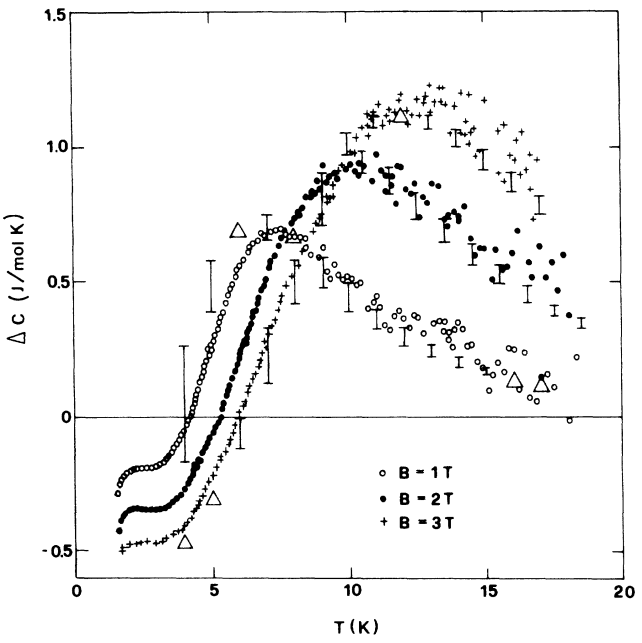

FIG. 5. Molar excess specific heat for CHAB. Open circles, solid circles, and crosses denote experimental data for $B=1,2,3$ T, respectively. The intercepts join the estimates obtained from linear and parabolic extrapolations. When extrapolations approximately coincide, the intercepts are substituted using triangles.

temperatures in order to avoid the overlap of the intercepts.

The results reported in Fig. 5 show an overall quantitative agreement with the measurements of ΔC. In the region of higher temperatures the theoretical results fit the experimental data from below. It is shown in Table III that in this region both linear and parabolic extrapolations have an upward tendency, so that we can consider our results as a lower bound. Because of that increasing tendency, it is likely that the results represented by the top of the intercepts are more reliable than those represented by the bottom.

We have also carried out zero-field specific-heat calculations with the parameters (3) appropriate for CHAC. The parameters (3) have been found in ferromagnetic resonance experiments,[4] and it is interesting to see whether they fit the previous specific-heat measurements.[2] The results of our numerical analysis with chains up to $N=12$ are reported in Fig. 1 using solid circles. In the low-temperature region, where some uncertainty is present, we report intercepts that join the estimates for the linear and parabolic extrapolations. The uncertainty is of the order 1% at $T\simeq 8$ K and rapidly decreases with increasing temperatures. Our results are rather accurate and reproduce fairly well the experimental data, apart from the height of the peak, which is largely determined by three-dimensional ordering. We conclude that the parameters (3) fit our theoretical predictions of the specific heat to the corresponding measurements. The present numerical results yield also the proper reference to our renormalization-group calculations.

IV. CONCLUDING REMARKS

In this paper we have presented two methods for the calculations of the specific heat of quantum spin chains: a real-space renormalization-group approach and a numerical approach via extrapolation of results for finite chains.

As for the renormalization-group approach, our zero-field specific-heat data for the XYZ model (Fig. 1) reveal qualitatively the experimental behavior of CHAC apart from the low-temperature region. Moreover, extending the calculations towards higher temperatures ($T>15$ K), we recover our accurate numerical estimates. Surprisingly, at higher temperatures the agreement with the numerical data (Fig. 1) is better than that found before for the XXZ model.[17]

If the in-plane field is applied, the excess specific heat of the easy-plane model shows the peak behavior (Figs. 2–4), which is observed experimentally for the soliton-bearing systems.[6,10,23] Our predictions are consistent with the appropriate measurements for CHAB. The peaks in question appear in most of the theories, although there are some exceptions.[24]

There is an inherent deficiency of our RSRG treatment that should be pointed out. If the external field is applied along the x direction, the x-y symmetry of the zero-order Hamiltonian is broken and the XXZ model is mapped by the RG transformation onto the XYZ model. In order to avoid this shortcoming, the external field can be put in the easy plane along the diagonal with respect to the x and y axis. The symmetry x-y is then preserved but the renormalization procedure generates a proliferation term of the type $S_i^x S_{i+1}^y + S_i^y S_{i+1}^x$. Taking into account the proliferation term, we do not find any substantial modification of the specific heat with respect to the results presented here in Sec. II.

Because of the symmetry of the Hamiltonian with respect to the inversion of the chain exploited here, we have extended the previous finite-size numerical calculations[6,13] up to $N=12$ as well as we have compared them with the zero-field specific-heat measurements for CHAC (Ref. 2) and the high-field measurements for CHAB.[6] The quantitative agreement with experiment has been found for most temperatures. An ambiguity appears at very low temperatures due to uncertainties in the extrapolations.

For CHAC, it is the first attempt to obtain reliable theoretical confirmation of the parameters (3). At first the specific-heat measurements[2] were interpreted within the easy-axis Heisenberg model by having recourse to the existing theoretical data.[3] Then the anisotropies have been obtained from resonance experiments,[4] whereas the value of the coupling constant remains controversial.

It is of interest, especially at low temperatures, to improve the extrapolation procedures, implementing, possibly, the series analysis ideas.[25] Some provisional Padè approximant estimates seem to be consistent with those obtained here for the linear extrapolations. However, we find again[26] a nonsystematic improvement of the Padè estimates with increasing temperature so that the problem deserves special attention and, possibly, an appropriate modification of the boundary conditions.

ACKNOWLEDGMENTS

We would like to thank Professor R. Dekeyser for his series analysis of our data and Professor F. Esposito for his assistance in the preparation of our computer program. One of us (G.K.) would like to acknowledge the Institute of Physics of the Lodz University for the partial support via project Centralung Program Badoir Podstawowych (CPBP) 01.08.

APPENDIX

We denote using ϵ_k and $|l_k\rangle$ the eigenvalues and eigenvectors of the free cell Hamiltonian $\mathcal{H}_{0i}$. Then we use the notations

$$a=\tfrac{1}{2}\sum_k e^{-\epsilon_k},\ b=\tfrac{1}{4}\sum_k e^{-\epsilon_k}\langle l_k|M^x|l_k\rangle ,$$

$$c=\tfrac{1}{2}\sum_k e^{-\epsilon_k}\langle l_k|\sigma^x_{i3}|l_k\rangle ,$$

$$\tilde{a}=a/(a^2-b^2),\ \tilde{b}=b/(a^2-b^2),\ d=-\tfrac{1}{2}\ln[(a+b)/(a-b)] ,$$

$$m=\frac{1}{2}\left[1+\frac{1}{4d}\sinh 4d\right],\ n=\frac{1}{2}\left[-1+\frac{1}{4d}\sinh 4d\right] ,$$

$$\pi^x=\sigma^x_{i3},\ \pi^y=-i\sigma^y_{i3},\ \pi^z=\sigma^z_{i3},$$

$$N^x=M^x ,\ N^y=-iM^y,\ N^z=M^z ,$$

$$\varphi(x)=(e^x-1)/x,\ N'=N/3 ,$$

$$R^{xx}=\tfrac{1}{4}\sum_k e^{-\epsilon_k}\sum_m \varphi(\epsilon_k-\epsilon_m)\langle l_k|\pi^x|l_m\rangle\langle l_m|N^x|l_k\rangle ,$$

$$Q^{\alpha\beta}_{\gamma\delta}=\tfrac{1}{16}\sum_{kl} e^{-\epsilon_k}e^{-\epsilon_l}\sum_m\sum_n \varphi(\epsilon_k-\epsilon_m+\epsilon_l-\epsilon_n)\langle l_k|\pi^\alpha|l_m\rangle\langle l_m|N^\beta|l_k\rangle\langle l_l|\pi^\gamma|l_n\rangle\langle l_n|N^\delta|l_l\rangle .$$

We can now give the recursion relations:

$$E'=\tfrac{1}{2}\ln(a^2-b^2)+\frac{K^x}{2}[(\tilde{a}c)^2-2\tilde{a}\tilde{b}cR^{xx}+\tilde{b}^2Q^{xx}_{xx}] ,$$

$$h'=\ln\frac{a+b}{a-b}+2K^x[-\tilde{a}\tilde{b}c^2+(\tilde{a}^2+\tilde{b}^2)cR^{xx}-\tilde{a}\tilde{b}Q^{xx}_{xx}] ,$$

$$K'^x=K^x(\tilde{b}^2c^2-2\tilde{a}\tilde{b}cR^{xx}+\tilde{a}^2Q^{xx}_{xx}) ,$$

$$K'^y=\frac{1}{m+n}[Q^{yy}_{yy}(m\tilde{a}^2-n\tilde{b}^2)+Q^{yz}_{yz}(m\tilde{b}^2-n\tilde{a}^2)]K^y+\frac{1}{m+n}[Q^{zz}_{zz}(-m\tilde{b}^2+n\tilde{Q}^2)+Q^{zy}_{zy}(-m\tilde{a}^2+n\tilde{b}^2)]K^z ,$$

$$K'^z=\frac{1}{m+n}[Q^{yy}_{yy}(n\tilde{a}^2-m\tilde{b}^2)+Q^{yz}_{yz}(n\tilde{b}^2-m\tilde{a}^2)]K^y+\frac{1}{m+n}[Q^{zz}_{zz}(-n\tilde{b}^2+m\tilde{a}^2)+Q^{zy}_{zy}(-n\tilde{a}^2+m\tilde{b}^2)]K^z .$$

*On leave of absence from the Institute of Physics, A. Mickiewicz University, 60-769 Poznan, Poland.

[1]J. D. Johnson and J. C. Bonner, Phys. Rev. B **22**, 251 (1980).

[2]K. Kopinga, A. M. C. Tinus, and W. J. M. de Jonge, Phys. Rev. B **25**, 4685 (1982).

[3]H. W. J. Blote, Physica (Utrecht) **79B**, 427 (1975).

[4]A. C. Phaff, C. H. W. Swuste, W. J. M. de Jonge, R. Hoogerbeets, and A. J. van Duyneveldt, J. Phys. C **17**, 2583 (1984).

[5]G. C. de Vries, E. Frikkee, K. Kakurai, M. Steiner, B. Dorner, K. Kopinga, and W. J. M. de Jonge (unpublished).

[6]K. Kopinga, J. Emmen, G. de Vries, L. F. Lemmens, and G. Kamieniarz, J. Phys. (Paris) Colloq. **49**, C8-1451 (1988).

[7]H. J. Mileska, J. Phys. C **11**, L29 (1978); **13**, 2913 (1980).

[8]E. Magyeri and H. Thomas, J. Phys. C **15**, L333 (1982).

[9]K. Kopinga, A. M. C. Tinus, and W. J. M. de Jonge, Phys. Rev. B **29**, 2868 (1984).

[10]A. M. C. Tinus, W. J. M. de Jonge, and K. Kopinga, Phys. Rev. B **32**, 3154 (1985).

[11]M. D. Johnson and N. F. Wright, Phys. Rev. B **32**, 5798 (1985).

[12]H. C. Fogedby, K. Osano, and H. J. Jensen, Phys. Rev. B **34**, 3462 (1986).

[13]G. Kamieniarz and C. Vanderzande, Phys. Rev. B **35**, 3341 (1987).

[14]I. Satija, G. Wysin, and A. R. Bishop, Phys. Rev. B **31**, 3205 (1985).

[15]G. M. Wysin and A. R. Bishop, Phys. Rev. B **34**, 3377 (1986).

[16]T. Delica, Phys. Rev. B **37**, 9879 (1988).

[17]L. S. Campana, A. Caramico D'Auria, U. Esposito, and G. Kamieniarz, Phys. Rev. B **39**, 9224 (1989).

[18]J. Sznajd, Z. Phys. B **62**, 349 (1986).

[19]R. C. Brower, F. Kuttner, M. Nauenberg, and K. Subbarao,

Phys. Rev. Lett. **38**, 1231 (1977).
[20]A. L. Stella and F. Toigo, Physica **89A**, 175 (1977).
[21]T. Schneider and E. Stoll, Phys. Rev. B **22**, 5317 (1980).
[22]F. Boersma, K. Kopinga, and W. J. M. de Jonge, Phys. Rev. B **23**, 186 (1981).
[23]A. P. Ramirez and W. P. Wolf, Phys. Rev. B **32**, 1639 (1985).
[24]R. W. Gerling and D. P. Landau, Phys. Rev. B **37**, 6092 (1988).
[25]P. M. Duxbury, J. Oitmaa, M. N. Barber, A. van der Bilt, K. O. Young, and R. L. Carlin, Phys. Rev. B **24**, 5149 (1981).
[26]G. Kamieniarz, Phys. Rev. B **38**, 4873 (1988).